Study of electron recombination in liquid Argon with the ICARUS TPC

ICARUS Collaboration

S. Amoruso [a], M. Antonello [b], P. Aprili [c], F. Arneodo [c],
A. Badertscher [d], B. Baiboussinov [e], M. Baldo Ceolin [e],
G. Battistoni [f], B. Bekman [g], P. Benetti [h], M. Bischofberger [d],
A. Borio di Tigliole [h], R. Brunetti [h], R. Bruzzese [a], A. Bueno [d,i],
M. Buzzanca [b], E. Calligarich [h], M. Campanelli [d],
F. Carbonara [a], C. Carpanese [d], D. Cavalli [f], F. Cavanna [b],
P. Cennini [j], S. Centro [e], A. Cesana [k], C. Chen [ℓ], D. Chen [ℓ],
D.B. Chen [e], Y. Chen [ℓ], K. Cieślik [m], D. Cline [n], A.G. Cocco [a],
Z. Dai [d], C. De Vecchi [h], A. Dąbrowska [m], A. Di Cicco [a],
R. Dolfini [h], A. Ereditato [a], M. Felcini [d], A. Ferrari [j,f], F. Ferri [b],
G. Fiorillo [a], S. Galli [b], Y. Ge [d], D. Gibin [e], A. Gigli Berzolari [h],
I. Gil-Botella [d], K. Graczyk [o], L. Grandi [h], A. Guglielmi [e],
K. He [ℓ], J. Holeczek [g], X. Huang [ℓ], C. Juszczak [o],
D. Kiełczewska [p,q], J. Kisiel [g], T. Kozłowski [q], M. Laffranchi [d],
J. Łagoda [p], Z. Li [ℓ], F. Lu [ℓ], J. Ma [ℓ], G. Mangano [a],
M. Markiewicz [m], A. Martinez de la Ossa [i], C. Matthey [n],
F. Mauri [h], G. Meng [e], M. Messina [d], C. Montanari [h],
S. Muraro [f], S. Navas-Concha [d,i], S. Otwinowski [n], Q. Ouyang [ℓ],
O. Palamara [c], D. Pascoli [e], L. Periale [r,s], G.B. Piano Mortari [b],
A. Piazzoli [h], P. Picchi [s,t,r], F. Pietropaolo [e], W. Półchłopek [u],
T. Rancati [f], A. Rappoldi [h], G.L. Raselli [h], J. Rico [d],
E. Rondio [q], M. Rossella [h], A. Rubbia [d], C. Rubbia [h], P. Sala [f,d],
R. Santorelli [a], D. Scannicchio [h], E. Segreto [b], Y. Seo [n],
F. Sergiampietri [v], J. Sobczyk [o], N. Spinelli [a], J. Stepaniak [q],
R. Sulej [w], M. Szarska [m], M. Szeptycka [q], M. Terrani [k],
R. Velotta [a], S. Ventura [e], C. Vignoli [h], H. Wang [n], X. Wang [a],
J. Woo [n], G. Xu [ℓ], Z. Xu [ℓ], A. Zalewska [m], C. Zhang [ℓ],
Q. Zhang [ℓ], S. Zhen [ℓ], W. Zipper [g]

[a] *Università Federico II di Napoli e INFN, Napoli, Italy*

[b] *Università dell'Aquila e INFN, L'Aquila, Italy*

[c] *INFN - Laboratori Nazionali del Gran Sasso, Assergi, Italy*

^{d}*Institute for Particle Physics, ETH Hönggerberg, Zürich, Switzerland*

^{e}*Università di Padova e INFN, Padova, Italy*

^{f}*Università di Milano e INFN, Milano, Italy*

^{g}*Institute of Physics, University of Silesia, Katowice, Poland*

^{h}*Università di Pavia e INFN, Pavia, Italy*

^{i}*Dpto de Física Teórica y del Cosmos & C.A.F.P.E., Universidad de Granada, Granada, Spain*

^{j}*CERN, Geneva, Switzerland*

^{k}*Politecnico di Milano (CESNEF), Milano, Italy*

$^\ell$*IHEP - Academia Sinica, Beijing, People's Republic of China*

^{m}*H.Niewodniczański Institute of Nuclear Physics, Kraków, Poland*

^{n}*Department of Physics, UCLA, Los Angeles, USA*

^{o}*Institute of Theoretical Physics, Wrocław University, Wrocław, Poland*

^{p}*Institute of Experimental Physics, Warsaw University, Warszawa, Poland*

^{q}*A.Sołtan Institute for Nuclear Studies, Warszawa, Poland*

^{r}*IFSI, Torino, Italy*

^{s}*Università di Torino, Torino, Italy*

^{t}*INFN Laboratori Nazionali di Frascati, Frascati, Italy*

^{u}*AGH-University of Science and Technology, Kraków, Poland*

^{v}*INFN, Pisa, Italy*

^{w}*Warsaw University of Technology, Warszawa, Poland*

Abstract

Electron recombination in Liquid Argon (LAr) is studied by means of charged particle tracks collected in various ICARUS Liquid Argon TPC prototypes. The dependence of the recombination on the particle stopping power has been fitted with a Birks functional dependence. The treatment of electron recombination in Monte Carlo simulations is discussed. A quantitative comparison with previously published data is carried out.

1 Introduction

Electron-ion recombination in liquid Argon ionization chambers has been studied by several experimental groups [1–5], both as a function of the electric field and as a function of the stopping power $(\frac{dE}{dx})$. However, the experimental conditions and the test particles were not the same in the different measurements, therefore a direct comparison is not straightforward. The drift field dependence has been studied with low energy electron or α sources, measuring the attenuation of the total collected charge. In this paper, we present data on recombination as a function of the stopping power obtained by the ICARUS collaboration analyzing stopping muon and proton tracks. In this case,

the signal attenuation is evaluated by comparing the measured and theoretical energy loss in small steps along particle tracks in the detector.

The approximations inherent to all the available theoretical models for recombination are discussed briefly. As a consequence, a phenomenological approach is used to parameterize the data, and Monte Carlo simulations are used to understand the relationship among the different data sets.

The ICARUS data for muons and protons, at drift fields ranging from 200 to 500 V/cm, are well described by Birks' law [6]. According to simulations, the ICARUS data are perfectly consistent with published electron data [1,2].

The ICARUS project [7] exploits the liquid Argon Time Projection Chamber (LAr TPC) technique [8], that allows three dimensional imaging of ionizing tracks. Ionization electrons produced in the detector active volume drift under the influence of an applied electric field toward parallel planes of wires having different orientations. Each wire plane provides a two-dimensional "view" of the ionizing event, with the position in one coordinate identified by the hit wire, and the time delay with respect to the trigger signal (internal or external) giving the position along the drift coordinate. The combined read-out of the wire "views" allows the three-dimensional reconstruction of the ionizing track. The signal amplitude provides a measurement of the collected charge.

The full scale ICARUS detector will consist of about 3000 tons of LAr, and will operate in the Gran Sasso underground laboratory as a high precision instrument for neutrino and rare event physics. Several small scale prototypes have been developed to test the technical issues related to the LAr TPC technique. We present here data from one of these, the so-called "3ton" chamber [3], and from the T600 [9] detector, which is the first module of the full ICARUS experiment.

2   Recombination models

As already pointed out in [10], none of the electron recombination theories developed so far is fully successful in describing all the experimental data in liquid Argon. Nevertheless, they provide the basis for its understanding and for all phenomenological approaches.

In the following, we will denote the initial ionization charge as Q_0, the collected charge as Q, related to Q_0 by the recombination factor $\mathcal{R}$, defined by $Q = \mathcal{R} \cdot Q_0$. $\mathcal{R}$ depends on the applied electric field $\mathcal{E}$ and on the density of the initial ionization. This last dependence is usually translated in a dependence on the $\frac{dE}{dx}$ for the ionizing particle. However, as we will discuss in the following, $\frac{dE}{dx}$ and ionization density are not fully equivalent.

2

Q_0 is related to the energy needed to produce an electron-ion pair. The world reference for this quantity in liquid Argon is $W_l = 23.6^{+0.5}_{-0.3}$ eV [11], deduced by extrapolation to infinite electric fields of the charge measured when a ^{207}Bi conversion electron source is immersed in a LAr ionization chamber. Assuming that all the energy E of the source particle is deposited in the detector, $W_l = E/Q_0$.

The Onsager [12] theory is based on the concept of "initial recombination" of the electron-ion pairs. It assumes that the electron has a finite probability of being captured back by the ion Coulomb field, and that this probability is reduced by the application of an external electric field. A simple expression for the recombination can be derived *for relatively low electric fields only*

$$Q = Q_0 e^{-\frac{r_{KT}}{r_0}} \left(1 + \frac{\mathcal{E}}{\mathcal{E}_{KT}}\right) \tag{1}$$

where $r_{KT} = e^2/\epsilon kT$, often referred to as the Onsager length, is the radius at which the electron thermal energy equals the Coulomb potential energy, and $\mathcal{E}_{KT}$ is such that $e\mathcal{E}_{KT}r_{KT} = kT$. $\mathcal{E}_{KT}$ is also the limit of applicability of Eq.1. The parameter r_0 is the average electron-ion distance at the end of the thermalization process, and is usually fitted to data as a free parameter. For a temperature $T \approx 90K$ and a dielectric constant $\epsilon = 1.53$ [13], one obtains $\mathcal{E}_{KT}$=1.3 kV/cm and $r_{KT} = 60$ nm. The Onsager theory does not consider the dependence on ionization density: it explicitly assumes a *single* electron/ion pair.

The Jaffè [14] "columnar" theory adopts a different approach. It assumes that the initial ionization charge is distributed in a "column" around the trajectory of the ionizing particle. Electrons and ions are supposed to drift away from this column under the effect of the external drift field and of charge diffusion. During the time evolution of the column, electrons can be captured by positive ions, with a probability proportional to the product of the charge densities. The resulting formula reads

$$Q = \frac{Q_0}{1 + q_0 F(\mathcal{E} \sin \phi)} \tag{2}$$

where q_0 is the initial density of electron-ion pairs, the function F also depends on the diffusion and mobility coefficients, and ϕ is the angle between the ionizing track and the electric field direction. For high electric fields (higher than 10 kV/cm in liquids [14]), $F \propto 1/\mathcal{E}$ and this is the dependence often used for the description of data.

Kramers [15] gives a modified version of the columnar theory, with a different treatment of diffusion. The formalism, although better grounded than Jaffè's, needs numerical integration to evaluate the recombination and contains an unknown factor that affects the low field behavior. The high field behavior is the same as in Jaffè's model.

Both approaches assume that electrons and positive ions drift with the same velocity,

and with a mobility which is independent of the electric field value.

Thomas and Imel [16] reinterpret the columnar equations assuming zero diffusion and zero ion mobility. To obtain analytical results, they replace the columnar boundary condition with the assumption of a uniformly distributed charge within a box (their model is known as the *box model*). The free charge is given by:

$$Q = Q_0 \frac{1}{\xi} ln(1 + \xi), \text{where} \quad \xi = \alpha \frac{Q_0}{\mathcal{E}} \tag{3}$$

and the parameter α is fitted to data. Note that $Q \to Q_0$ for $\mathcal{E} \to \infty$.

It has to be pointed out that all the above "columnar-like" theories assume a direct proportionality between the electron drift velocity and the applied electric field. This approximation fails in LAr for drift fields higher than a few hundreds of $\frac{V}{cm}$, while most experimental data are taken at several $\frac{kV}{cm}$. Despite of this inherent limitation, the functional form of the box model and the asymptotic form of the Jaffè theory are often successfully used to fit experimental data. Indeed, Jaffè's formulation is usually approximated with the so-called Birks [6] law, that is also used for the description of quenching effects in scintillators:

$$Q = \frac{Q_0}{1 + k_E/\mathcal{E}} \tag{4}$$

where $\mathcal{E}$ is the applied electric field and k_E is a constant to be fitted to data. Eq. 4 implies that $\mathcal{R} \to 1$ in the limit of infinite field. The same functional dependence is normally also used to describe the recombination as a function of the particle stopping power $\frac{dE}{dx}$:

$$Q = \frac{Q_0}{1 + k_Q \frac{dE}{dx}} \tag{5}$$

By combining the two last relations with the Columnar theory, one obtains

$$k_Q(\mathcal{E}) = \frac{k}{\mathcal{E}} \tag{6}$$

3   Published data

Most measurements of electron-ion recombination in liquid Argon essentially investigated the dependence of recombination on the electric field. They were performed by measuring the total charge deposited by electrons or alpha particles from sources immersed in small LAr ionization chambers.

In this paper, we will consider in particular the measurements of Scalettar et al. [1], and those of Aprile et al. [2].

The Scalettar et al. experiment measured the signal induced by a ^{113}Sn conversion electron source (364 keV electrons) and by a ^{241}Am source (5.6 MeV α) in LAr with drift fields from 0.075 kV/cm to 9 kV/cm; it is labeled in this paper by a subscript S.

The Aprile et al. experiment (subscript A) measured the 976 KeV electron line of ^{207}Bi in a similar electric field range.

4   ICARUS Data

4.1   The 3ton prototype

The ICARUS 3ton [3] prototype was operated at CERN and collected data from cosmic rays and radioactive sources with different drift fields. It was equipped with two perpendicular wire planes having a pitch of 2 mm. The liquid Argon temperature was 92 K, corresponding to a density $\rho = 1.36$ g/cm^3 [17].

Charge collection along stopping muon and stopping proton tracks was analyzed at drift fields of 200, 350 and 500 V/cm (the corresponding data are labeled $3t$ in the following). The variation of $\frac{dE}{dx}$ with the energy allows to determine the recombination factor for different stopping powers, (from the ionization minimum (m.i.p) to about 30 MeV/(g/cm^2)) simply dividing the particle tracks into suitable steps. Details of the chamber set-up and of the data analysis can be found in [3]. Only the results for stopping muons were included in that paper [1]. Here, we reanalyze and add the proton data. This allows for a much longer lever arm and therefore for a better determination of the Birks k_Q parameter.

4.2   The T600 detector

The ionization along stopping muon tracks was also studied with the first ICARUS T600 technical run.

One half of the T600 was equipped with two TPCs sharing a common cathode. Each TPC includes three wire planes, with wires at $\pm60°$ and $0°$ with respect to the horizontal. The wire pitch is 3 mm. The drift field was set to 500 V/cm and the maximum drift distance is about 1.5 m. The liquid Argon temperature during the data taking was 89 K, corresponding to a density $\rho = 1.38$ g/cm^3. The trigger was provided either

---

[1]   Values obtained at 500 V/cm are labeled by mistake as "700 V/cm" in Fig. 18 and in the Birks fits of ref. [3].

by an internal system of photomultipliers detecting the LAr scintillation light, or by external scintillator planes.

A detailed description of the detector and of the data taking can be found in [9]. Other experimental results obtained in the T600 test run are given in [18,19]. A complete description of charge collection and signal extraction can be found in [19]. The procedure to measure $\mathcal{R}$ is summarized in the following, and described in detail in [20,21].

Stopping muons were visually identified among cosmic ray events. The muon tracks were reconstructed with the automatic procedure and the energy at each position evaluated from the range to the decay point. All tracks were divided into segments whose length is energy dependent and is chosen in order to obtain the best estimate of $\frac{dE}{dx}$. The event sample was divided into events for which the timing of the track with respect to the trigger (and hence the absolute value along the drift coordinate) is known, referred to as *in-time* events, and events for which this information is unknown (*out-of-time* tracks). For in-time events, the collected charge was corrected for the measured drift electron attachment to impurities according to the experimentally determined drift electron lifetime (around 1.3 ms, depending on the data taking period, for a maximum drift time of about 1 ms). $\mathcal{R}$ for m.i.p.'s was computed as the ratio between the measured and theoretically expected value of the most probable value of the Landau distribution, for track segments of a fixed length and minimal expected $\frac{dE}{dx}$. The uncertainty on the measurement is dominated by the error on the drift electron lifetime and the length of the track segments, and amounts up to 2%. For out-of-time events, the absolute time of the event was derived comparing the average energy loss far from the decay point to the same quantity for the in-time sample. The systematic error associated to this procedure was evaluated by applying it to the in-time event sample, and may be translated into a 7% contribution to the energy resolution.

In order to measure the recombination at different stopping powers, muon segments were grouped according to the theoretical stopping power (expected mean energy loss given by the Bethe-Bloch formula estimated from the range to the muon decay point). For each $\frac{dE}{dx}$ bin the value of $\mathcal{R}$ was computed as the ratio between the mean measured and theoretical stopping power.

All collected charge values were corrected for a non perfect transparency of the wire planes [2] . The correction factor as evaluated with electric field calculations is 1.10±0.05.

---

[2] For a discussion of the wire plane transparency, see Ref.[3]. During the technical run of the T600, the wire chambers were biased to +280,0,-220 V, resulting to a non perfect transparency across the middle wire plane.

6

Data Set	particle		topic	$\mathcal{R}$ at 0.5 kV/cm
3ton	stopping	μ, p	$\mathcal{R}_{3t}$ vs $\frac{dE}{dx}$	mip : 0.70 ± 0.02
			3 $\mathcal{E}$ values	
Scalettar [3]	^{113}Sn source	364 keV e^-	$\mathcal{R}_S$ vs $\mathcal{E}$	0.58 ± 0.01
	^{241}Am source	5.64 MeV α	$\mathcal{R}_\alpha$ vs $\mathcal{E}$	$0.014 \pm ?$
Aprile [4]	^{207}Bi source	976 keV e^-	$\mathcal{R}_A$ vs $\mathcal{E}$	0.64 ± 0.05
T600	stopping	μ	$\mathcal{R}_{T600}$ vs $\frac{dE}{dx}$	mip : 0.71 ± 0.04

Table 1

Summary of available recombination data

5 Data comparison

The 3ton and T600 recombination factors ($\mathcal{R}_{3t}$ and $\mathcal{R}_{T600}$) for different fields and stopping powers are shown in Figs. 1 and 2. The other two sets of data $\mathcal{R}_S$ and $\mathcal{R}_A$ (reconstructed from the published plots) are shown in Fig. 3, where we also add for comparison the $\mathcal{R}_{3t}$ value for minimum ionizing particles. According to the original papers, we assume an error of ± 0.02 fC for all the electron data from ref. [1], and a common systematic error of 7% for data in [2]. Data set features are summarized in Table 1.

At the field of interest for ICARUS (0.5 kV/cm) the recombination values are:

$$\mathcal{R}_S = 0.58, \quad \mathcal{R}_A = 0.64, \quad \mathcal{R}_{3t} = 0.70 \quad \mathcal{R}_{T600} = 0.71 \tag{7}$$

In principle, one expects a difference in the recombination factor between m.i.p. tracks and electron full energy deposition. While it is true that 0.36 and 0.94 MeV electrons are minimum ionizing particles at the beginning of their paths, it is also true that their stopping power increases as soon as they slow down. Even simply dividing the total energy by the CSDA range [22], one obtains an average stopping power of 2.4 MeV/(g/cm^2) for the 364 keV electrons, vs 1.5 MeV/(g/cm^2) for a minimum ionizing muon. The non-linearity of electron recombination with respect to $\frac{dE}{dx}$ may enhance this difference. A quantitative analysis will be carried out in the following.

6 Birks and Box model fits

As mentioned before, both the Birks and the Box models have been employed to describe recombination, letting k or ξ as free parameter to be fitted to the data. In both cases, the recombination should be governed by the ratio $\frac{q_0}{\mathcal{E}}$.

In Fig. 4 we show the percentage difference between data and fit for the Scalettar electron data and the two models. All points have been included in the fit. It is clear that the two models have very similar accuracy at high fields, and very similar inaccuracy (more than 20%) at low fields. This is not surprising, since they use similar theoretical assumptions and the same approximation on the drift velocity. Indeed, the Birks fit to $\mathcal{R}_S$ presented in the original paper [1] includes only the points at $\mathcal{E} > 2$ kV/cm and if extrapolated to low fields does not match to the experimental data. Both models agree better with the low field region data if an additional normalization parameter A is added:

$$Q = A \frac{Q_0}{1 + k/\mathcal{E} \frac{dE}{dx}} \tag{8}$$

Fitting $\mathcal{R}_S$ data up to 1.5 kV/cm with the Birks law the normalization is $A_S = 0.83 \pm 0.01$

The same trend is found when fitting the data as a function of the stopping power: a normalization factor different from one is needed to obtain good agreement. This becomes evident when plotting $1/\mathcal{R}$ vs $\frac{dE}{dx}$, as in Fig.5 for the 3ton data. According to Eq.8, all the $1/\mathcal{R}$ points at a given field should lie on a straight line: this is remarkably true for all the three electric field conditions. It is also evident that the lines do not have an intercept at $1/\mathcal{R} = 1$. A similar behavior is seen for the electron data when $1/\mathcal{R}_S$ is plotted vs $1/\mathcal{E}$ (Fig. 6). The linearity is fulfilled only for small electric field ranges, with slope and intercept depending on the field value. The line on the plot is the Birks law with $k_E = 0.53$ kV/cm as in the original paper.

However, for a limited electric field range the combined dependence of recombination on the ratio $\frac{dE/dx}{\mathcal{E}}$ is very well verified. This is shown in Fig.7 for all the 3ton data rescaled according to the different drift fields.

An overall Birks fit to $\mathcal{R}_{3t}$ at all fields gives:

$$A_{3t} = 0.800 \pm 0.003, \quad k_{3t} = 0.0486 \pm 0.0006 \text{ kV/cm} \frac{\text{g/cm}^2}{\text{MeV}} \quad (k_Q = \frac{k}{\mathcal{E}}) \tag{9}$$

Corresponding to $k_Q = 0.097 \pm 0.001 \frac{\text{g/cm}^2}{\text{MeV}}$ at 0.5 kV/cm, in good agreement with the value in [3].

For the T600 data at 500 V/cm, the small lever arm leads to a larger uncertainty in the k_Q parameter: we obtain $k_Q = 0.11 \pm 0.01 \frac{\text{g/cm}^2}{\text{MeV}}$, with a normalization $A_{T600} = 0.81 \pm 0.05$. These values are compatible with the one obtained for the 3ton data. A summary of the fitted Birks parameters is presented in table 2.

Besides the non constant mobility, other reasons for the deviations from the Birks law have been put forward, for instance the co-presence of Onsager and Jaffè effects, or the

8

Data Set	particle	$\mathcal{E}$ range $\frac{\text{kV}}{\text{cm}}$	A	k $\frac{\text{kV}}{\text{cm}}\frac{\text{g}}{\text{cm}^2\text{MeV}}$	k_E $\frac{\text{kV}}{\text{cm}}$
3ton	μ, p	0.25-0.5	0.800±0.003	0.0486± 0.0006	
Scalettar	364 keV e^-	0.075-1.5	0.83± 0.01		0.179± 0.003
T600	μ	0.5	0.81±0.05	0.055± 0.005	

Table 2

Summary of fitted Birks parameters. The fit to Scalettar et al. data has been limited to $\mathcal{E} < 1.5$ kV/cm to allow for a comparison with the ICARUS data.

different recombination of the low energy δ rays produced along and not experimentally separable from the primary track [23].

The latter topic, δ rays, deserves more consideration. It has already been partially investigated in [23,24], in relation to the observed energy resolution in LAr. The model fits to $\mathcal{R}$ vs ionization density are all performed (not only for LAr, also for scintillators) assuming that the recombination depends on the *total* stopping power, implicitly assuming that the energy is uniformly deposited around the particle track. In reality, δ rays are produced and quenched according to their stopping power. What is experimentally observed is a "dressed" track. Even assuming perfect columnar recombination, the real "signal" Q due to an initial charge Q_0 should be written as a sum over several ionization contributions:

$$Q = \sum_i \frac{Q_{0i}}{1 + k_Q \frac{dE}{dx}_i}, \quad \sum_i Q_{0i} = Q_0 \tag{10}$$

which is different from the "bare" track

$$Q = \frac{Q_0}{1 + k_Q \frac{dE}{dx}} \tag{11}$$

The difference cannot be easily estimated. Very low energy electrons will fall within the "column", medium energy ones will be highly quenched, high energy δ are minimum ionizing at the beginning, but strongly ionizing at the end of their range. The net effect depends on the energy spectrum of the produced δ rays, on the "original" recombination, on the total stopping power etc.

Therefore, the Birks or Box laws should be regarded as purely phenomenological curves useful to model the data. Moreover, it is clear that the high recombination region, that means either low electric fields or high ionization density, cannot be easily matched to the low recombination region. This is why we do not include here a discussion on recombination for alpha particles: at the highest drift field for which published data exist, (30 kV/cm) the ratio $\frac{dE}{dx}/\mathcal{E}$ is of the order of 20. This corresponds to $\mathcal{E} \approx$ 0.1 kV/cm for a minimum ionizing particle, or even less if the saturation of drift velocity plays a role.

9

In the following, we will adopt the Birks description for both data and simulations. In this way, we keep open the possibility to explore with a dedicated experimental setup a possible dependence on the track angle with respect to the drift field. This dependence is foreseen in the Jaffè model and not in the box model.

7 Monte Carlo simulations

The effect of quenching has been simulated with the FLUKA [25] Monte Carlo code, to quantitatively understand the different values of $\mathcal{R}$ for the various data sets, and to find a reliable quenching description for the ICARUS simulations in general. Since, however, the treatment of ionization energy loss and recombination are based on the same principles in most transport Monte Carlo codes, the considerations expressed here are of more general concern.

Ionization energy losses in FLUKA are subdivided in a continuous part and in a δ-production part. δ-rays are produced only above a kinetic energy threshold (T_δ) set by the user. The continuous energy loss part includes fluctuations.

A quenching algorithm can be activated in the simulation. Each energy deposition is quenched according to a Birks law with a given set of input parameters. From the discussion in the previous section it is clear that this can in principle lead to inconsistencies, since a global quenching parameter derived for a global energy deposition is separately applied both to the continuous and the δ energy depositions. We expect possible discrepancies with respect to experimental recombination factors, and a dependence on T_δ.

As a first step, the experimentally determined parameters of expression 9 have been used as input for the simulation. The response to minimum ionizing particles (250 MeV kinetic energy muons) has been simulated for different values of T_δ. Results are shown in Fig. 8. Over-quenching up to 17% is observed for very low T_δ, a small under-quenching for intermediate thresholds, and again over-quenching where the absence of δ rays is compensated by large fluctuations in the continuous energy loss.

There are in principle different approaches to resolve this effect:
• Try to be "as microscopic as possible", that is to set T_δ such that only electrons with a range smaller than a "columnar radius" are kept in the continuous energy loss. This approach does not work because of two reasons. First, what we obtain from data is a "dressed" recombination coefficient, not the "bare" one; second, the "columnar radius" in liquids is of the order of tens of nm [14,15]. This clashes with both CPU time constraints and the validity range of transport models.
• Adjust the quenching coefficient at each step in the Monte Carlo transport, taking into account that there are different components of the energy loss, in order to get the

correct overall recombination. In other words, let the k_B in the sum of Eq. 10 as free parameters and calculate them during the simulation in such a way to have the same Q of Eq.11. However, since δ rays are randomly generated and followed like any other particle, this would need either an a-priori knowledge of the history that has to be simulated, or a pre-tabulation as a function of the particle type, its energy, T_δ and so on.

• Adopt an empirical approach. Choose the best T_δ on the basis of the needed simulation accuracy, and find a set of Birks parameters that, applied to all simulated energy loss, with this specific threshold, reproduce the data. This method has been tested and implemented in our MonteCarlo simulation.

In all ICARUS simulations, the δ threshold (and the electron transport threshold) is set to 10 keV (corresponding to an electron range of about 3 μm). This is also a reasonable value to simulate the energy deposition from electron sources. With this value the over-quenching for m.i.p. in Fig 8 is of the order of 6% when the parameters from the 3ton data are used.

The recombination factor has been calculated with this threshold for muons and protons, for different values of the Birks parameter k_{in}, ranging from 0.5 to 1.5 of the nominal experimental one k_{nom}. For each input k_{in}, a linear fit of $1/\mathcal{R}$ vs $\frac{dE}{dx}$ gives an "effective" Birks parameter k_{eff}, and a Monte Carlo normalization constant A_{MC}. The aim is to obtain $k_{eff} = k_{nom}$, in order to have the correct slope of the quenching, and then recalibrate the Monte Carlo results with a factor A_{exp}/A_{MC} to obtain the experimental values.

All Monte Carlo sets are well fitted by the Birks law. The fitted k_{eff} shows a linear dependence on the input k_{in}, as shown in Fig. 9. Since the contribution of δ rays leads to an over-quenching of minimum ionizing particles, while for highly ionizing particles the effect is smaller (few δ) or even opposite (δ's have a smaller $\frac{dE}{dx}$ than the parent particle) the net effect is a reduction of the effective slope with respect to the input one.

The result is that in order to obtain the slope of the experimental data ($k_{eff} = k_{nom} = 0.098$ (g/cm^2)/MeV) the input parameter must be

$$k_{in} = 0.1225 \ (\text{g/cm}^2)/\text{MeV}$$

And the Monte Carlo calibration factor results to be

$$\frac{A_{exp}}{A_{MC}} = 0.8/0.92 = 0.87$$

The correspondence between $\mathcal{R}_{MC}$ and $\mathcal{R}_{3t}$ with these input parameters is shown in Fig. 10.

8 Simulation results

We can use the simulations described in the previous section to check the consistency among the different experimental data sets.

Using the input Birks parameters derived above, we obtain for $\mathcal{E} = 0.5$ kV/cm:

$$\text{Data} \qquad \mathcal{R}_S = 0.58, \quad \mathcal{R}_A = 0.64 \quad \mathcal{R}_{3t} = 0.70$$

$$\text{Monte Carlo} \quad \mathcal{R}_S = 0.58, \quad \mathcal{R}_A = 0.64 \quad \mathcal{R}_{3t} = 0.69$$

with an agreement that is better than the experimental uncertainty.

As described in the previous sections, we do not expect that the Birks parametrization of the 3ton data can be extended to much higher fields than the ones entering in the fit. To test the validity limit, we compared the Scalettar data with the Monte Carlo simulation assuming $k = k_Q/\mathcal{E}$. The agreement is excellent up to $\mathcal{E} < 0.7$ kV/cm. At 1 kV/cm the simulated value is lower than data by $\approx 5\%$, at 2 kV/cm the difference is around 10%.

We also tested the response to 5.64 MeV α particles from ^{241}Am, although we do not expect the Birks law to hold over a stopping power range from 1.5 to 500 MeV/cm. The experimental value from ref [1] is $\mathcal{R}_\alpha = 0.014$, and the simulation result is $\mathcal{R}_\alpha = 0.011$.

9 Conclusions

Cosmic-ray data collected with the 3ton and T600 ICARUS TPC detectors allowed for a precise determination of the recombination factor in liquid Argon. Data have been fitted to a Birks law as a function of the particle stopping power and of the drift electric field. The agreement between data points and the fitted functions is remarkably good, although the many approximations embedded in the columnar theory of recombination prevent the direct extrapolation to a wide range of electric fields.

From the 3ton data we obtain for the recombination parameter the value $k = 0.0486 \pm 0.0006$ (kV/cm)(g/cm^2)/MeV in the range $0.1 < \mathcal{E} < 1.$ kV/cm, $1.5 < \frac{dE}{dx} < 30$ MeV/(g/cm^2). For the normalization factor we obtain $A = 0.800 \pm 0.003$. The T600 data give an independent confirmation of these results, even though with less statistical significance. The extrapolation to very high ionization density, as those obtainable with α particles, is accurate at the 30% level. Consistency with published data has been verified by means of dedicated Monte Carlo simulations based on the FLUKA code.

10   Acknowledgments

References

[1] R.T. Scalettar et al., Phys. ReV. **A 25**, 2419 (1982).

[2] E. Aprile et al., Nucl. Instr. Meth. **A 261**, 519 (1987).

[3] P. Cennini et al., Nucl. Instr. Meth. **A 345**, 230 (1994).

[4] C. R. Gruhn and M. D. Edmiston, Phys. Rev. Lett. **40**, 407 (1978).

[5] E. Shibamura et al., Nucl. Instr. Meth. **A 260**, 437 (1987).

[6] J. Birks, Theory and Practice of Scintillation Counting, Pergamon Press, 1964.

[7] ICARUS Collaboration, CERN/SPSC 2002-027, LNGS-EXP 13/89 add. 2/01.

[8] C. Rubbia, *The Liquid-Argon Time projection Chamber: a new concept for Neutrino Detector*, CERN-EP/77-08, (1977).

[9] ICARUS Collaboration, *The ICARUS T600 Detector*, in preparation.

[10] E. Barrelet *et al.* [H1 Calorimeter Group Collaboration], Nucl. Instrum. Meth. A **490** 204 (2002).

[11] M. Miyajima et al., Phys. ReV. **A 9**, 1438 (1974).

[12] L. Onsager, Phys. ReV. **54**, 554 (1938).

[13] "CRC Handbook of Chemistry and Physics", D.R Lide ed., (CRC Press)

[14] G. Jaffé, Ann. Phys. **42**, 303 (1913).

[15] H. A. Kramers, Physica 18, 665 (1952).

[16] J. Thomas and D.A. Imel, Phys. ReV. **A 36**, 614 (1987).

[17] S. Angus and B. Armstrong, "International thermodynamic tables of the fluid State", Butterworths, London, 1972

[18] F. Arneodo et al. [ICARUS collaboration], Nucl. Inst. Meth., **A 508**, 287 (2003).

[19] S. Amoruso et al. [ICARUS Collaboration], "Analysis of the liquid Argon purity in the ICARUS T600 TPC" Accepted for publications by NIM A.

[20] J. Rico, PhD thesis, Diss. ETH No. 14906, (2002) see http://neutrino.ethz.ch/diplomathesis.html .

[21] S. Amoruso et al. [ICARUS Collaboration], " Measurement of the μ decay spectrum with the ICARUS liquid argon TPC", in preparation.

[22] M.J. Berger,1 J.S. Coursey and M.A. Zucker, Berger, M.J., Coursey, J.S., and Zucker, M.A. (1999), *ESTAR, PSTAR, and ASTAR: Computer Programs for Calculating Stopping-Power and Range Tables for Electrons, Protons, and Helium Ions (version 1.2.2)* (1999) Available: http://physics.nist.gov/Star National Institute of Standards and Technology, Gaithersburg, MD.

[23] E. Aprile et al., IEE trans. on Nucl. Sci. **35**, 37 (1988).

[24] D.A. Imel, J. Thomas, Nucl. Instr. Meth. **A 273**, 291 (1988).

[25] A. Fassò, A. Ferrari, J. Ranft and P.R. Sala, "FLUKA: Status and Perspectives for Hadronic Applications" , Proc. of the Monte Carlo 2000 Conference, Lisbon, 23-26 October 2000, A. Kling et al. eds. ,(Springer, Berlin, 2001); A. Fassò, A. Ferrari, J. Ranft and P.R. Sala, "Electron-photon transport in FLUKA: status", Proc. of the Monte Carlo 2000 Conference, Lisbon, 23-26 October 2000, A. Kling et al. eds. ,(Springer, Berlin, 2001).
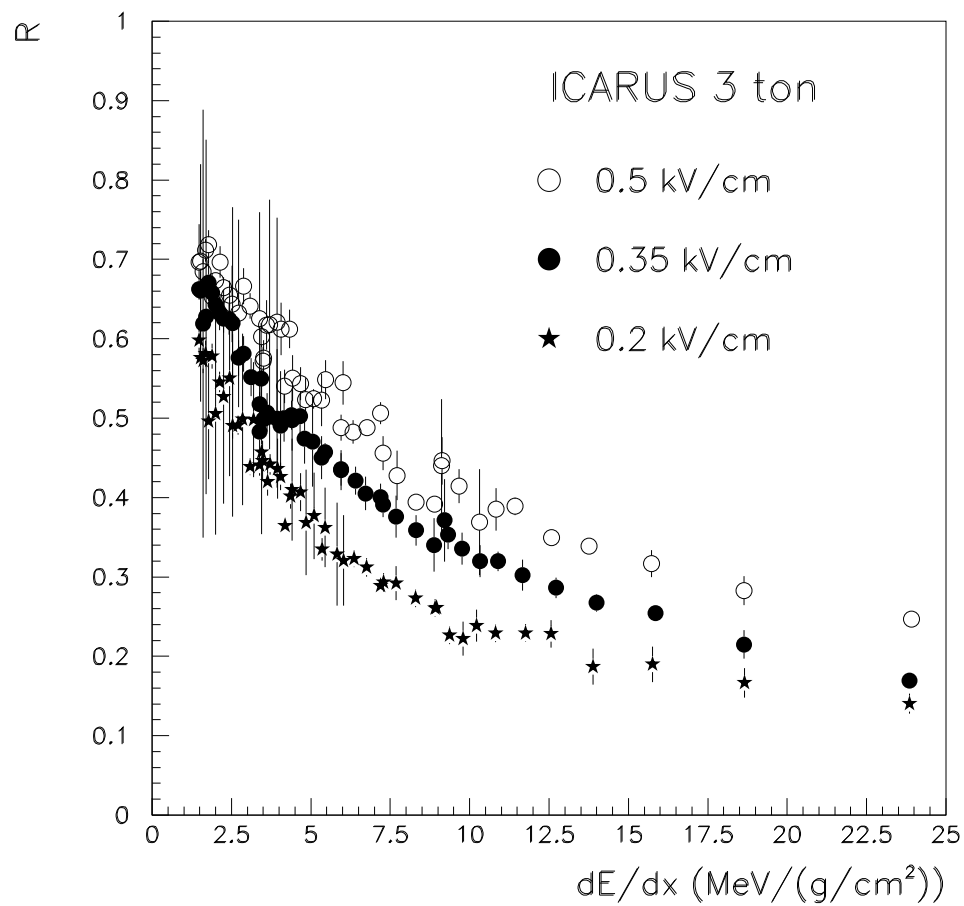
Fig. 1. Recombination factors measured with the 3 ton ICARUS prototype as a function of the theoretical particle stopping power (see text), for different electric field values.
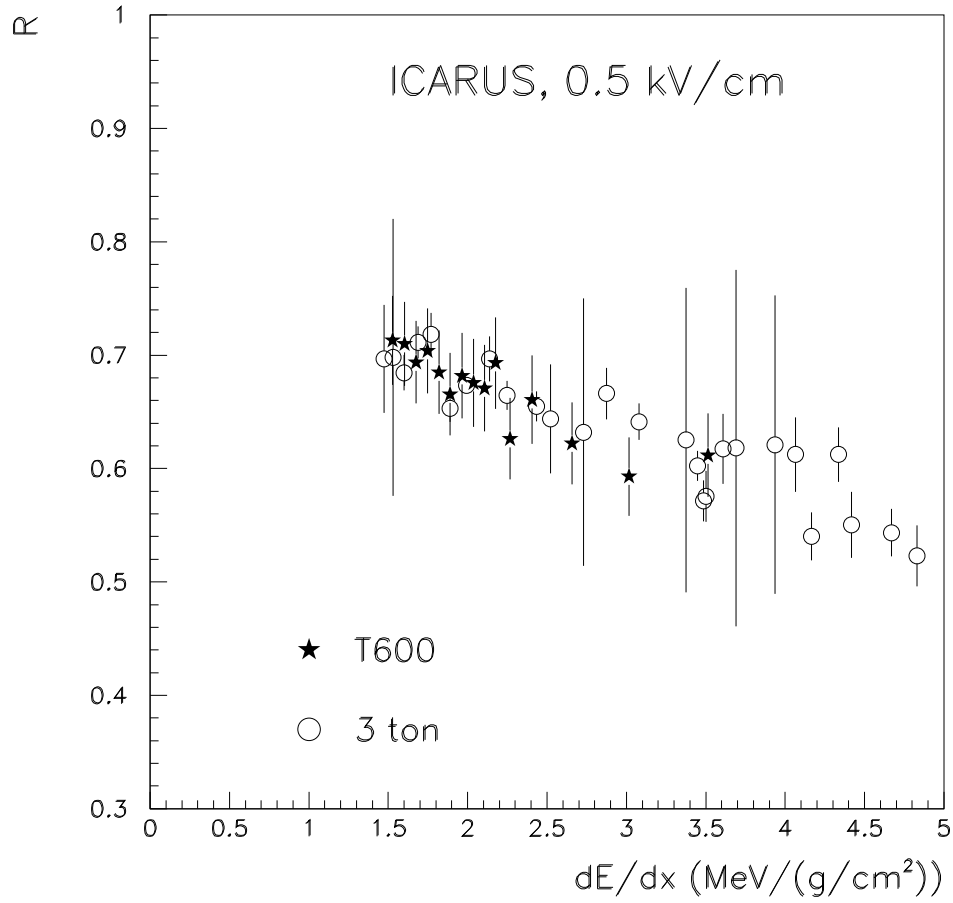
Fig. 2. Recombination factors measured with the ICARUS T600 and 3 ton detectors at 500 V/cm as a function of the theoretical particle stopping power (see text). The errors on T600 data include a 5% systematics from the transparency correction.
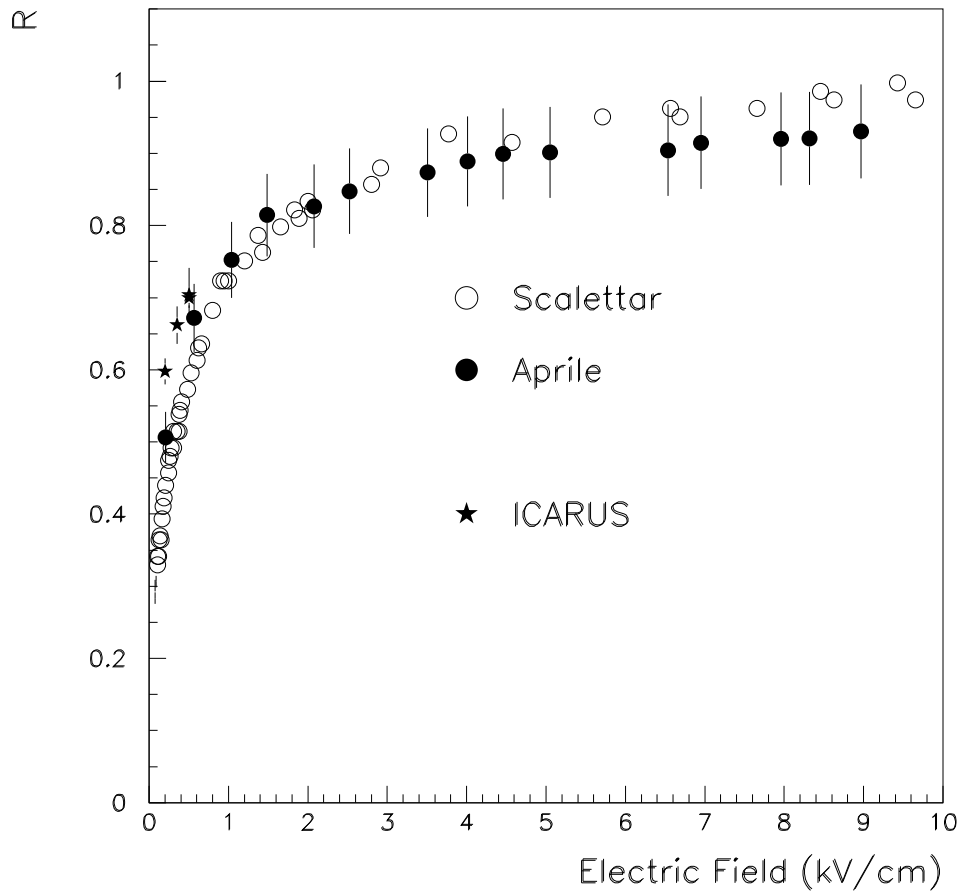
Fig. 3. Recombination factors as a function of the electric field, for 364 keV electrons [1], 976 KeV electrons [2], and minimum ionizing particles (ICARUS, this work). Errors on the Scalettar et al. data are smaller than the symbol size.

17
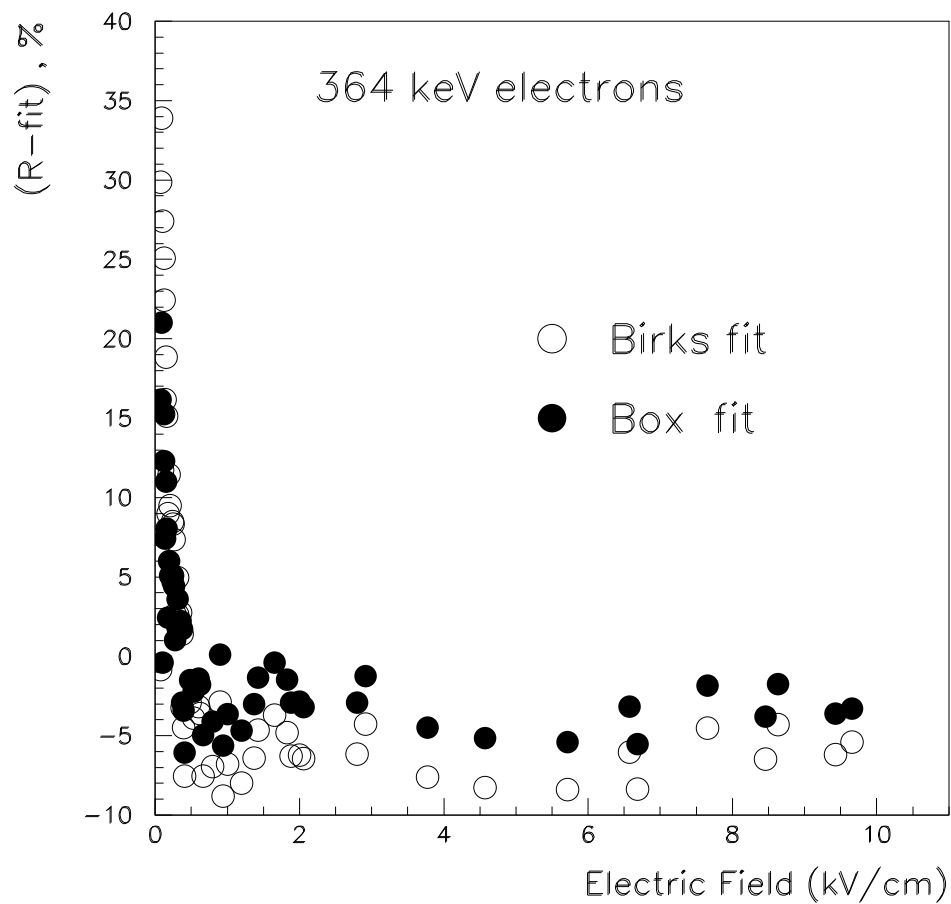
Fig. 4. Percentage difference between data (Scalettar et al.) and Birks or Box fits to all points, keeping the normalization fixed to one (see text).
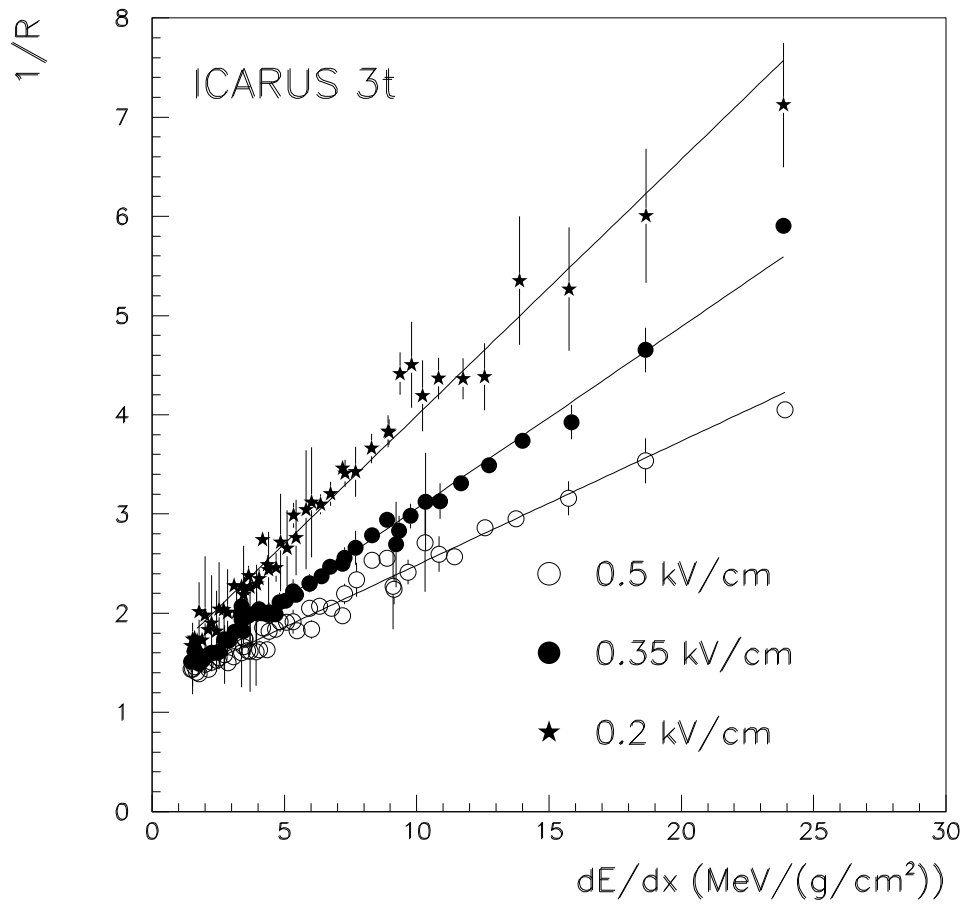
Fig. 5. Birks fit of the inverse of the recombination factor vs. stopping power. Data are from the 3ton prototype at different electric fields
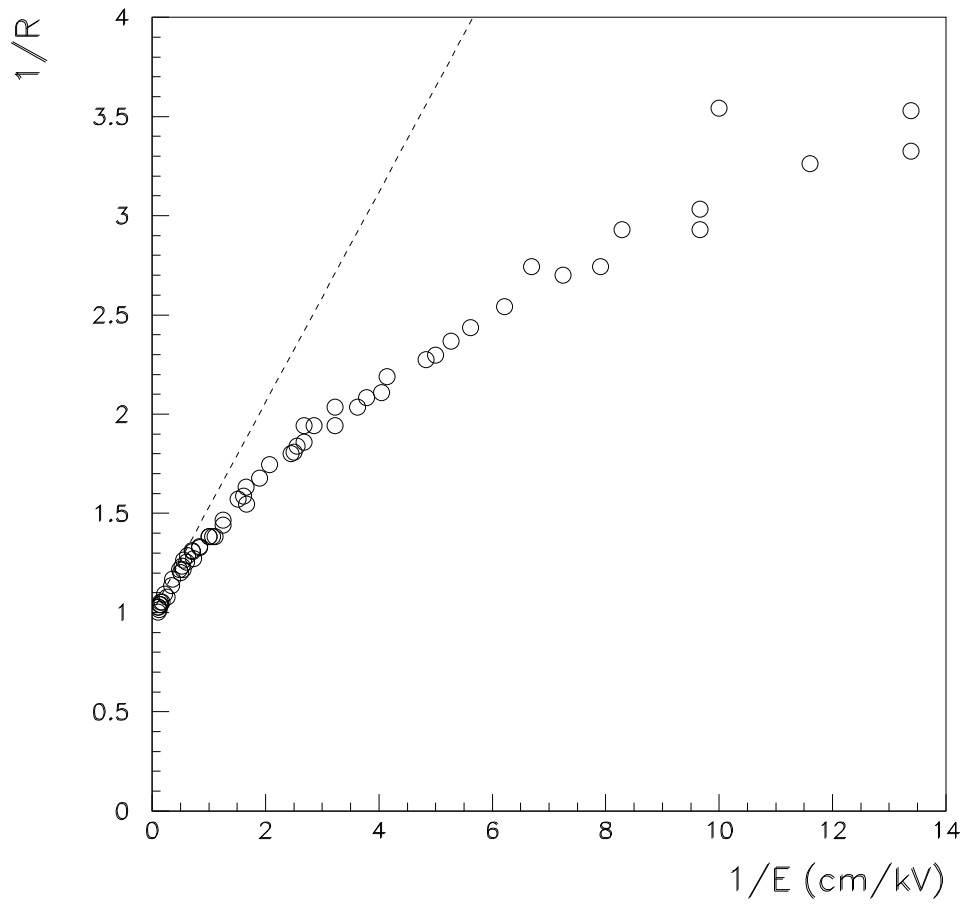
Fig. 6. "Linearized" plot of the data from [1]. The dashed line is the Birks fit to the data for E>2 kV/cm (as in [1]).
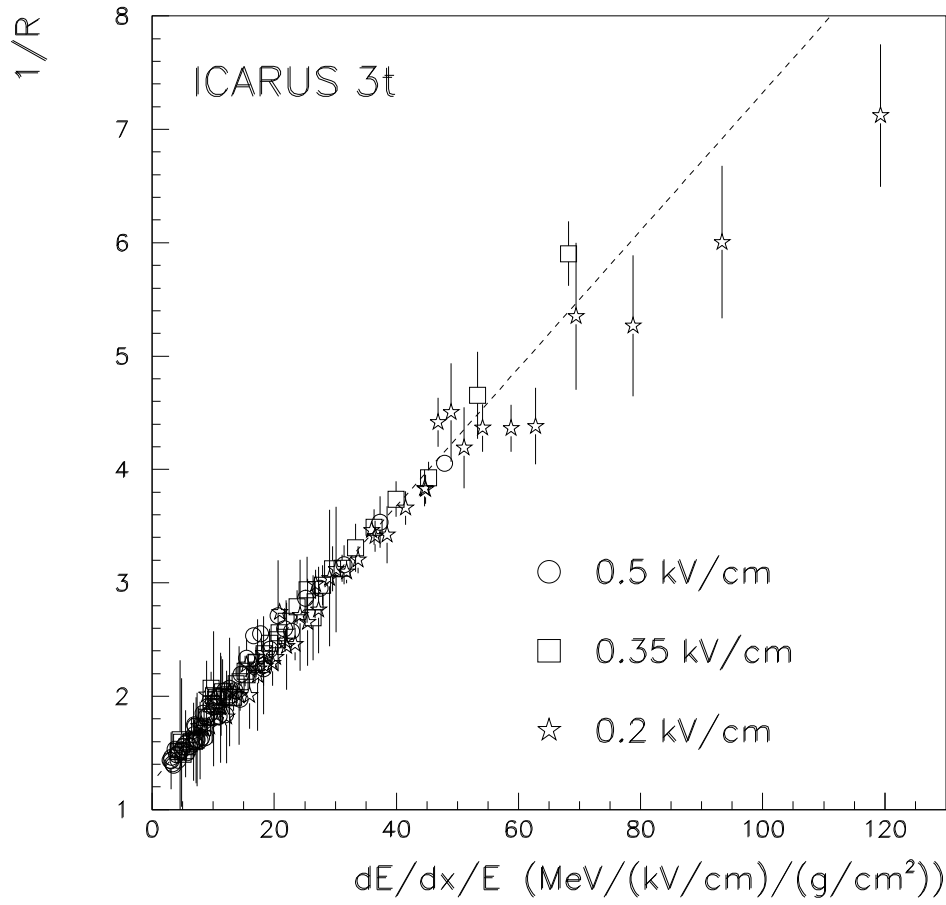
Fig. 7. Birks fit of the inverse of the recombination factor vs. stopping power divided by the electric field value. Data are from the 3ton prototype for different electric fields values.
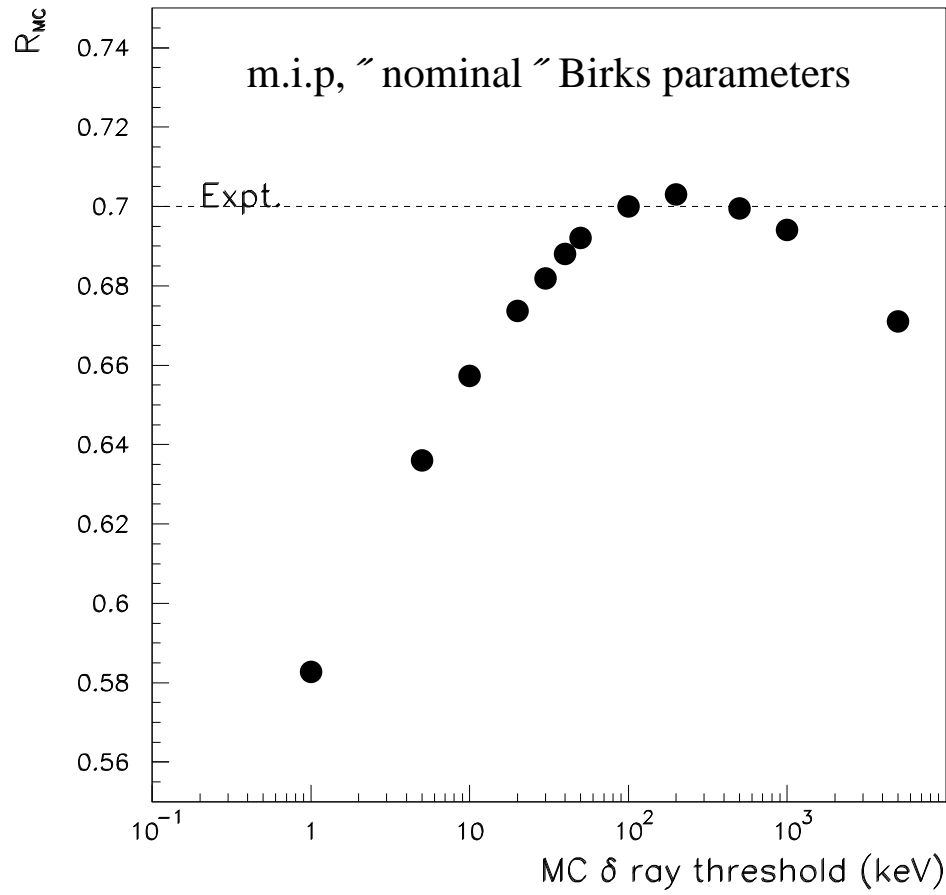
Fig. 8. Monte Carlo recombination factor as a function of the δ ray production threshold. The Birks parameters as extracted from the 3ton data fit are directly used in the simulation (see text for details). The line corresponds to the experimental value.
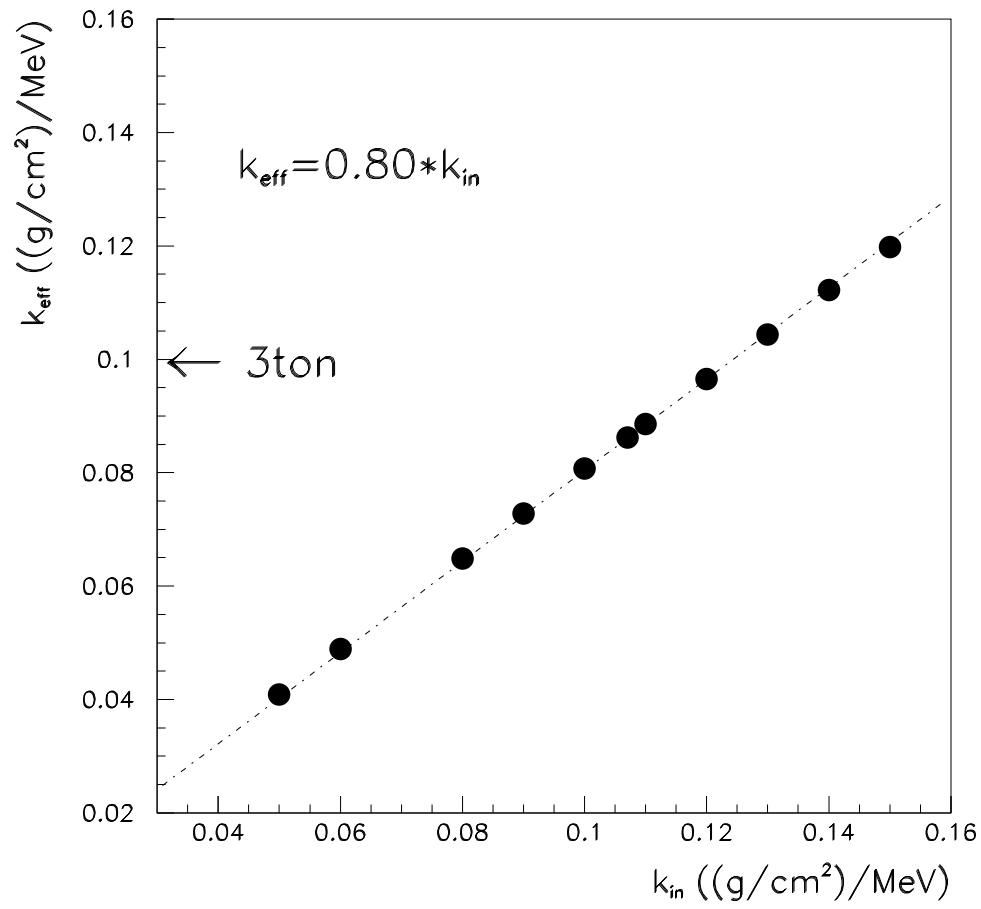
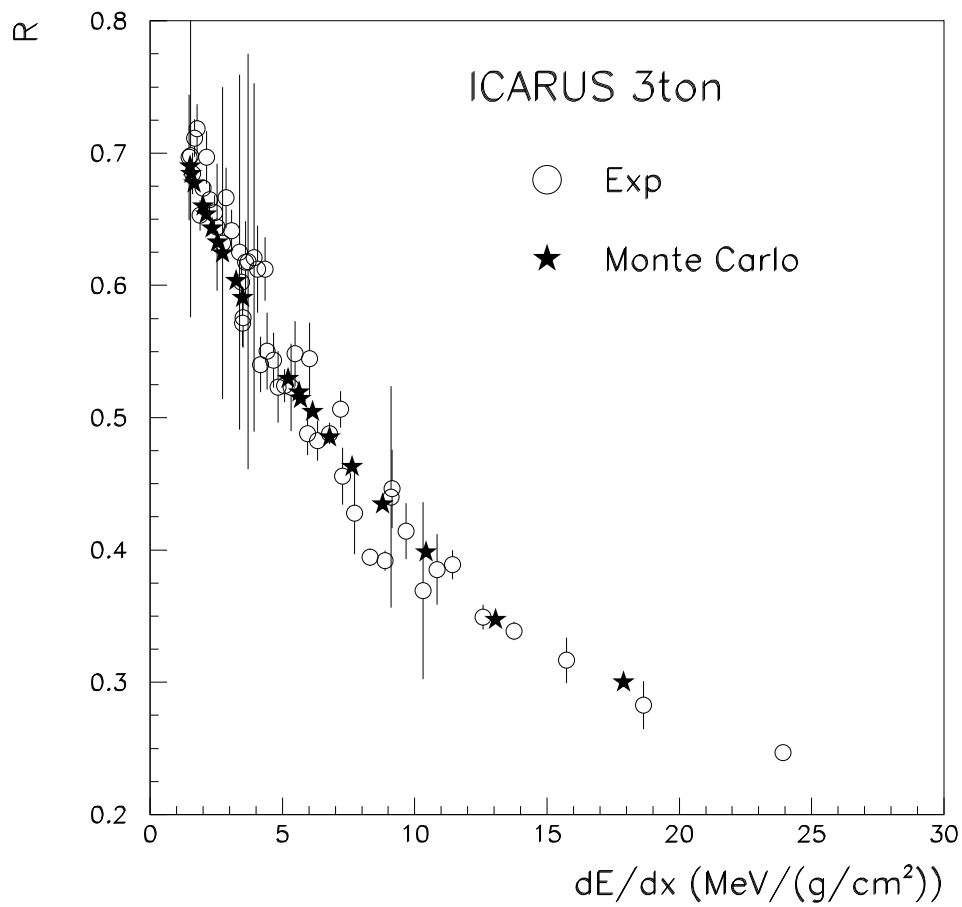Fig. 9. Effective Monte Carlo Birks coefficient as a function of the input Birks coefficient

Fig. 10. Experimental and Monte Carlo recombination factors with the input Birks parameters as determined in this work.